



Effect of Liquid Load Level and Binder Type on the Tableability of Mesoporous Silica Based Liquisolds

Jan Appelhaus¹ · Kristina E. Steffens¹ · Karl G. Wagner¹

Received: 16 May 2024 / Accepted: 24 September 2024
© The Author(s) 2024

Abstract

Mesoporous silica offers an easy way to transform liquids into solids, due to their high loading capacity for liquid or dissolved active ingredients and the resulting enhanced dissolution properties. However, the compression of both unloaded and loaded mesoporous silica bulk material into tablets is challenging, due to poor/non-existing binding capacity. This becomes critical when high drug loads are to be achieved and the fraction of additional excipients in the final tablet formulation needs to be kept at a minimum. Our study aimed to investigate the mechanism of compression and tableability dependent on the Liquid Load Level of the silica and type of filler/binder in binary tableting mixtures. To this end, Vivapur® 101, FlowLac® 90, Pearlitol® 200 SD and tricalcium citrate tetrahydrate were selected and mixed with Syloid® XDP 3050 at various Liquid Load Levels. Compaction characteristics were analysed using the StylOne® Classic 105 ML compaction simulator. Additionally, the Overall Liquid Load (OLL) was defined as a new critical quality attribute for liquisolid tablets. The Overall Liquid Load allows straightforward, formulation-relevant comparisons between various fillers/binders, liquid components, and silica types. Results indicate strong binding capacity and high plasticity of the fillers/binders as key components for successful high liquid load silica tablet formulation. A volumetric combination of 30% Vivapur® 101 and 70% 0.75 mL/g loaded Syloid® XDP 3050 proved to be the most effective mixture, achieving an Overall Liquid Load of 36–41% [v/v] and maintaining a tensile strength of 1.5 N/mm² with various liquid vehicles.

Keywords Liquid Load Level · Liquisolid · Mesoporous silica · Overall Liquid Load · Tableting

Introduction

Silica is a versatile material extensively used in the pharmaceutical industry for various applications. Primarily, it is used as a glidant, but it can also be utilised as a desiccant or serve as a carrier for actives in solid or liquid form [1, 2]. Silica can be classified into two types, non-porous fumed silica (such as Aerosil® or Carb-O-Sil®) and mesoporous silica, with a pore size ranging from 2–50 nm [3]. Mesoporous silica can be further categorised into ordered and disordered types based on their pore structure [4].

“Liquisolid systems” were developed in the 1990s by Spireas *et al.*, [1, 5] and have shown promising results in increasing the solubility of drugs exhibiting poor aqueous solubility. This is especially important since with the advent

of high throughput screening methods, more new chemical entities are poorly water-soluble [6]. In literature, increased *in vitro* solubility has been described for cannabidiol [7], naproxen [8], furosemide [9], carbamazepine [10], and several other active pharmaceutical ingredients (APIs) [11–13]. Additionally, some authors also report successful *in vivo* trials with both beagle dogs [14] and healthy human volunteers [15].

Liquid components such as hydrophobic vitamins [16], N,N-dimethylacetamide [17], propylene carbonate [18], polyethylene glycol 400 [19], polysorbate 80 [20] or propylene glycol [21] can be successfully incorporated into liquisolid systems. The successful loading of these chemically diverse liquid components shows that, utilising liquisolid technologies, both lipo- and hydrophilic solvents and APIs can successfully be transformed into liquisolid systems.

According to Spireas *et al.*, [1, 5], “liquisolid systems” are apparently dry, non-adherent and readily compressible powdered forms of liquid medications. Such a liquisolid system is based on a relatively large porous carrier material,

✉ Karl G. Wagner
karl.wagner@uni-bonn.de

¹ Department of Pharmaceutics, University of Bonn,
Gerhard-Domagk-Str. 3, 53121 Bonn, Germany

such as microcrystalline cellulose, in which pores are filled with a drug solution up to the level, that a thin film forms on the outer surface. The latter drastically reduces the carrier's flowability. Subsequently, this excess drug solution is absorbed by a very fine ($d = 10\text{--}5000\text{ nm}$) coating material, such as various types of fumed silica, which are adsorbed in mono- or multilayers on the surface of the carrier material to bind the excess liquid and thus restore flowability. The carrier-to-coating ratio is recommended to be around 20:1 [1, 5].

In a liquisolid system, maximising total liquid load is crucial, because the maximum achievable dose within a reasonable volume depends on both the solubility of the API in the liquid and the maximum liquid loading into the carrier. This limiting factor has been identified as a major drawback for liquisolid technologies [22], even as the use of newer carrier materials enabled higher liquid loads [16]. However, it is problematic to accurately compare the currently achieved total liquid loads, as the information on loading quantities is usually only given on a mass basis. Due to the different densities of drug solutions and excipients, these values are not accurately comparable. Therefore, further optimisation was needed to enable liquisolids as a viable formulation principle from a key performance indicator as well as a formulation standpoint.

Mesoporous silica generally has a high maximum loading capacity, which can increase the total possible liquid loading [23]. However, mesoporous silica also poses some challenges. It has poor tableting properties [3], which necessitates the addition of a filler/binder. Certain silica grades such as Syloid® 244FP also exhibit very low bulk density, thus limiting direct tableting. Others, like Silsol® 6035, are restricted as their maximum loading capacity is below 0.75 mL/g. Syloid® XDP 3050 on the other hand provides a high bulk density and retains excellent flow properties up to its maximum absorption capacity of 1.6 mL/g. Up to this value no coating material to maintain good flow properties is required [23]. Recent debates have arisen regarding the definition of liquisolid systems in literature, particularly concerning whether wet, non-flowable forms of liquisolids are nonetheless considered a “liquisolid system” [24, 25]. Due to the lack of coating material, the liquid-loaded Syloid® XDP 3050 presented in this study is technically not a “liquisolid system” by the original patent [5]. However, ever since the original patent had been published, most authors define a “liquisolid” as an apparently dry, non-adherent, free-flowing and compressible powder. Therefore, the blends presented in this study are considered liquisolids by common definition [16, 26].

Our study aimed to investigate the binding properties of Syloid® XDP 3050 at different Liquid Load Levels [v/m]. Our first objective involved finding an optimal filler/binder. Initial investigations revealed that compacts of pure

silica violently tare themselves apart upon exiting the die when silica is not loaded, while no bonds are formed at the maximum Liquid Load Level. Our second objective is two-fold: to optimise the maximum liquid loading using patient- and formulation-relevant parameters, while simultaneously achieving a tensile strength of $1.5 \pm 0.1\text{ N/mm}^2$ for the resulting tablets.

Materials and Methods

Materials

Syloid® XDP 3050 was used as the mesoporous silica, and propylene carbonate as the liquid component for the preparation of liquisolids during the investigation. The silica was provided by Grace GmbH (Germany), and the propylene carbonate was purchased from VWR International S.A.S. (France). The fillers/binders Vivapur® 101, FlowLac® 90, tricalcium citrate tetrahydrate and Pearlitol® 200SD were kindly provided by JRS Pharma GmbH & Co. KG (Germany), Meggle GmbH & Co. KG (Germany), Jungbunzlauer GmbH (Germany) and Roquette Frères S.A. (France), respectively. The die was lubricated using Ligamed MF-2 V magnesium stearate kindly donated by Peter Greven GmbH & Co. KG (Germany). Propylene carbonate was dyed using methylene blue by Merck (Germany). Polyethyleneglycol 400 (PEG400) was purchased from Carl Roth GmbH (Germany), propylene glycol (PG) from Fagron GmbH & Co. KG (Germany) and polysorbate 80 (PS80) from Caesar & Loretz GmbH (Germany).

Methods

Preparation of Liquisolids

The incipient wetness method was utilised to create liquisolids with Liquid Load Levels of 0 mL/g, 0.5 mL/g, 1.0 mL/g, and 1.5 mL/g of propylene carbonate. The process involved adding the liquid component to pre-dried Syloid® XDP 3050, which had subsequently been stirred with a spatula until no lumps were visible [27]. Finally, to ensure a homogeneous distribution, the powder was mixed at 50 rpm for 10 min in a turbula mixer (Willi A. Bachofen AG, Switzerland). For other liquids than propylene carbonate, the same procedure was utilized.

Filler/Binder Selection

Preliminary experiments have shown that pure Syloid® XDP 3050 and liquisolids cannot form tablets without adding further excipients while operating at realistic tableting speeds. Vivapur® 101, FlowLac® 90, Pearlitol® 200SD,

and tricalcium citrate tetrahydrate were selected as fillers/binders for this study, as all of them tend to form tablets of adequate tensile strength (TS) but also differ in their deformation and bonding behaviour.

Bulk, Tapped and Helium Pycnometer Density

Bulk (V_{Bulk}) and tapped densities (V_{Tapped}) of all liquisols and our chosen fillers/binders were determined. Therefore, 50 mL of powder was filled into a graduated cylinder and weighed accurately. The cylinder containing the powder was transferred to a tapped density tester, and the test was performed according to the regulations of the Ph. Eur. 10.0, 2.9.34, method one [28], with reduced volume. All measurements were performed in triplicate. The Hausner ratio (H_R) was calculated to assess the flow character according to Ph. Eur. 10, Table 2.9.36–2.

$$H_R = \frac{V_{\text{Bulk}}}{V_{\text{Tapped}}} \quad (1)$$

The helium pycnometer densities of the unmixed powders were measured using a Belpycno L (Microtrac Retsch GmbH, Germany) helium pycnometer. The chamber of the pycnometer was purged five cycles before analysis. A fill pressure of 200 kPa and an equilibration rate of 0.08 kPa/min were employed. Measurements were repeated until five subsequent cycles had a standard deviation below 0.1%. Before analysis, the excipients were dried at 75 °C for 30 min. All measurements were performed in triplicate. The helium pycnometer densities of the liquisols were calculated from the values of the unloaded silica and the density of the liquid component. That is because solvent vapours could damage the device.

$$\rho_{\text{HP}(l)} = \frac{(V_{l/g} * \rho_L) + 1}{V_{l/g} + (1 \div \rho_{\text{HP}(s)})} \quad (2)$$

where $\rho_{\text{HP}(l)}$ is the helium pycnometer density of the liquisolid, $V_{l/g}$ the volume of liquid per gram of silica, ρ_L the density of the loaded liquid and $\rho_{\text{HP}(s)}$ the helium pycnometer density of the pure, dry silica.

Using the values obtained from equation 2, the helium pycnometer densities of the binary mixtures ($\rho_{\text{HP}(m)}$) could be calculated according to Eq. 3.

$$\rho_{\text{HP}(m)} = \frac{(\phi_l * \rho_{\text{Bulk}(l)}) + (\phi_b * \rho_{\text{Bulk}(b)})}{((\phi_l * \rho_{\text{Bulk}(l)}) \div \rho_{\text{HP}(l)}) + ((\phi_b * \rho_{\text{Bulk}(b)}) \div \rho_{\text{HP}(b)})} \quad (3)$$

where ϕ_l and ϕ_b are the volume parts based on bulk volume, $\rho_{\text{Bulk}(l)}$ and $\rho_{\text{Bulk}(b)}$ the bulk densities, and $\rho_{\text{HP}(l)}$ and $\rho_{\text{HP}(b)}$ the helium pycnometer densities of liquisolid and filler/binder respectively.

Design of Experiments (DOE)

A Full Factorial Design of Experiments with three centre points was created for each filler/binder using MODDE® 13 (Sartorius Stedim Biotech GmbH, Germany) with the compaction pressure (250 MPa, 350 MPa, 450 MPa), silica content (0%, 70%) and Liquid Load Level (0 mL/g, 1.5 mL/g) of propylene carbonate as factors. Tensile strength and Overall Liquid Load (OLL) were chosen as responses. The latter represents the percentage of liquid volume to the overall tablet volume and therefore signifies a new critical quality attribute for liquisolid tablets, as the amount of liquid per unit determines the possible drug load for a given liquid API or saturated drug solution. Multi-linear regression was used to fit the models. The DOE software optimiser enabled maximisation of the Overall Liquid Load while maintaining a tensile strength of $1.5 \pm 0.1 \text{ N/mm}^2$.

Preparation of Binary Mixtures

To ensure a consistent silica surface as a contact area for bonding, the binary mixtures were formulated using bulk volume ratios rather than mass ratios. This was necessary due to the significant increase in bulk density observed with increasing Liquid Load Level of the liquisols. In total, 30 mL of each mixture was prepared. All ingredients were mixed in a turbula mixer (Willi A. Bachofen AG, Switzerland) for 10 min with a rotation of 50 rpm.

Tabletting

Binary mixtures were compressed into tablets using 8 mm flat tooling on a StylOne® classic 105ML single punch tablet press (Medelpharm, France, Romaco Kilian, Germany). The press was equipped with external displacement sensors calibrated to $\pm 5 \mu\text{m}$ as well as internal pressure sensors. All tablets were produced using the default compression cycle at 10% speed, resulting in a 30 ms dwell time and an overall compression cycle of 650 ms. The die was manually filled and externally lubricated with magnesium stearate. In total, five tablets per binary mixture were produced. A binary mixture was considered defective if more than one tablet showed capping or delamination, or if the tablets were too fragile to be picked up with tweezers after compression. In this case, concerning the DOE, the silica content of the mixture was lowered by 10% until a stable mixture had been achieved. Afterwards, the respective MODDE® values were adjusted accordingly.

Out-of-Die Analysis

The height (Mitutoyo Absolute ID C125B, Mitutoyo Corp., Japan) and weight (AG 204, Mettler Toledo GmbH,

Germany) of the tablets were determined immediately after compression. Additionally, after 24 h of storage at 20 °C and ambient humidity, the height of the tablets was measured again before proceeding to crushing force testing (Erweka TBH 200, Erweka GmbH, Germany). Using this data, the tensile strength, solid fraction, and Overall Liquid Load of each tablet were calculated. Tensile strength is a normalisation of a tablets crushing force and therefore is independent of its geometry for biplanar round tablets [29].

$$TS = \frac{2 * F}{\pi * d * h} \quad (4)$$

where F is the crushing force, d the diameter and h the height of the tablet.

Solid fraction (SF) represents the apparent density (ρ_{App}) of the compact with respect to its true density. In our case, the helium pycnometer density was used as a close approximation of the true density. SF can be calculated from the helium pycnometer density of the binary mixture ($\rho_{HP(m)}$) used, the tablet weight (m_{Tab}), height (h_{Tab}), volume (V_{Tab}) and radius (r).

$$SF = \frac{\rho_{App}}{\rho_{HP(m)}} \quad (5)$$

$$\rho_{App} = \frac{m_{Tab}}{V_{Tab}} \quad (6)$$

$$V_{Tab} = \pi * r^2 * h \quad (7)$$

As described above, the Overall Liquid Load (OLL) is the percentage of liquid volume to the overall tablet volume.

$$\omega_s = \frac{(V_{Bulk(l)} * \rho_{Bulk(l)})}{(V_{Bulk(l)} * \rho_{Bulk(l)}) + (V_{Bulk(b)} * \rho_{Bulk(b)}) + \sum (V_{Bulk(n)} * \rho_{Bulk(n)})} \quad (8)$$

$$\omega_l = \frac{V_{l/g} * \rho_l}{(V_{l/g} * \rho_l) + 1} \quad (9)$$

$$OLL = \frac{((m_{Tab} * \omega_s * \omega_l) \div \rho_l)}{V_{Tab}} \quad (10)$$

where ω_s is the mass fraction of the loaded silica of the tablet, $V_{Bulk(l)}$ is the bulk volume fraction of the liquisolid, $\rho_{Bulk(l)}$ is the bulk density of the liquisolid, $V_{Bulk(b)}$ is the bulk volume fraction of the filler/binder, and $\rho_{Bulk(b)}$ is the bulk density of the filler/binder. $V_{Bulk(n)}$ and $\rho_{Bulk(n)}$ represent the volume fraction and bulk density of all other additional components of the blend, if present. ω_l is the mass fraction of the liquid in the loaded silica, $V_{l/g}$ the Liquid Load Level and ρ_l the density of the liquid.

Full-Screening

In addition to the DOE, further binary mixtures (Electronic supplementary material A-1) were prepared for all fillers/binders using propylene carbonate as the liquid component. Mixtures were produced as described above and compressed into tablets at 250 MPa, 350 MPa and 450 MPa using the same compression cycle as the DOE.

After completing the out-of-die measurements, the resulting data were analysed using a custom Python script featuring the matplotlib library [30]. A contour plot was created to visualise both the tensile strength and Overall Liquid Load data for each filler/binder/compaction pressure combination, plotted against the silica content of the binary mixture and the Liquid Load Level. This allowed for the accurate identification of all blends with a certain tensile strength from the respective contour plot using Python by varying the contour levels. This contour line can subsequently be transferred onto the Overall Liquid Load contour plot, as they share the same X and Y axis, to optimise the Overall Liquid Load for a specific tensile strength.

Optimised Formulations

The optimal Liquid Load Level, silica content, filler/binder, and pressure combination predicted via the full-screening method for each filler/binder were produced and tested using the methods described above. Apart from propylene carbonate, propylene glycol, PEG400 and polysorbate 80 were tested as liquid components with the most suitable filler/binder found during previous experiments to determine if results can be reproduced using various liquids at the same mixing ratio. If tensile strength results were below the target of $1.5 \pm 0.1 \text{ N/mm}^2$, filler/binder content was increased by 5% [v/v] until sufficient tensile strength was reached for each liquid. As the higher filler/binder content might allow for higher compression pressures, the compression pressure was also adjusted in the case of a formulation adjustment.

Compaction Behaviour of Silica and Liquisolds without Binder/Filler

Syloid® XDP 3050 was loaded with 0, 0.5, 1.0 and 1.5 mL/g of methylene blue-dyed propylene carbonate. These liquisolds were subsequently compressed with 200 MPa of pressure using the same tooling, tablet press, sensors and compression cycle described in Sect. "Tabletting". Preliminary experiments had shown that stable compacts could not be achieved at all tested Liquid Load Levels. To obtain the desired tablet weight, the powder was weighed before compression. If possible, the resulting tablet or its fragments were collected after compression and weighed again. Measurements were performed in triplicate.

Tab-Fox Analyser (Mathias Hucke Software, Germany) was used to calculate the reference energy of compaction from the external displacement data. This reference energy (E_{Ref}) can be divided into reorganisation energy (E_1), compaction energy (E_2), elastic recovery energy (E_3) and plastic flow energy (E_4).

$$E_{Ref} = E_1 + E_2 + E_3 + E_4 \quad (11)$$

$$E_{Ref} = \frac{(FH - d_{min}) * F_{max}}{2} \quad (12)$$

where FH is the fill height, d_{min} is the minimal distance and F_{max} is the average maximum force of the upper and lower punch achieved during compaction.

The compaction energy (E_2) can be calculated from the force height data collected during the compression cycle. The work done by both punches over the compression stroke represents the upper limit of energy available for bond formation during the compaction process, with some energy being lost by die-wall friction.

$$E_2 = \int_{x=0}^{x_{max}d} [(F_{Up} + F_{Lp}) \div 2] * dx_d \quad (13)$$

F_{Up} and F_{Lp} are the upper and lower punch forces measured during compression. To comply with the common graphical representation, $x=0$ is the filling depth, and x the travel distance of the punches, representing the compression of the powder bed plotted in the positive direction.

To compare different compaction energies, they can be normalised by the reference energy to calculate the compaction ratio:

$$\text{Compaction Ratio} = \frac{E_2}{E_{Ref}} \quad (14)$$

Additionally, the tableting behaviour of Syloid® XDP 3050 was analysed at the four chosen Liquid Load Levels using the model equation by Kawakita [31]. It describes the volume reduction of a powder in linearised form, where a and b are the model parameters, P is the applied pressure and C is the relative volume decrease.

$$\frac{P}{C} = \frac{P}{a} + \frac{1}{ab} \quad (15)$$

The relative volume decrease at pressure P can be calculated from the bulk density $\rho_{Bulk(L)}$ and the apparent density ρ_P at pressure P [32].

$$C = 1 - \left(\frac{\rho_{Bulk(L)}}{\rho_P} \right) \quad (16)$$

The parameter a represents the degree of compression at infinite pressure. The parameter b^{-1} mathematically

represents the pressure required to reach $a/2$. Therefore, b^{-1} may reflect the initial compressibility (or deformation capacity) of a powder [33].

The bulk modulus (K) can be determined via the pressure difference (Δp) and the volume change (ΔV) after exceeding the pycnometer density, as well as the tablet volume (V).

$$K = -V \frac{\Delta p}{\Delta V} \quad (17)$$

Extended Dwell Time Measurements

Syloid® XDP 3050 was loaded with 0, 0.5, 1.0 and 1.5 mL/g of methylene blue-dyed propylene carbonate. These liquisolid s were compressed at 200 MPa using a StylOne® classic 105ML (Medelpharm, France) single punch tablet press with 8 mm round flat face tooling and external displacement sensors calibrated to $\pm 5 \mu\text{m}$. The compaction cycle was modified to a dwell time of 30 s. The compaction simulator stops any further compression upon reaching the set compaction pressure for the first time. During compression, the top of the die and the viable part of the upper punch were visually monitored for any external liquid leakage. The force-height data, force-time data, and plastic flow energy (E_4) were analysed using Tab-Fox Analyser (Mathias Hucke Software, Germany). The plastic flow energy is delivered to the tablet by the tensioned machine over the dwell time after the maximum force has been reached. It represents the capacity of a material for further compression under sustained load.

$$E_4 = \int_{x_{max}F}^{x_{min}d} [(F_{Up} + F_{Lp}) \div 2] * dx_d \quad (18)$$

where E_4 is the plastic flow energy, F_{Up} and F_{Lp} are the upper and lower punch forces measured during compression and x is the distance between both punches.

Results

Bulk, Tapped and Helium Pycnometer Density

An overview of the measured densities and flow characteristics for all tested powders is presented in Table I. Silica flowability progressively improved with an increase in Liquid Load Level. All compounds and binary mixtures exhibited sufficient flowability for the manual die-filling process during tableting.

Table 1 Bulk, tapped and helium pycnometer densities (ρ_{HP}), Hausner ratio (H_R) and Ph. Eur. 10.0 flow character of Liquisols and fillers/binders used.

Excipient	ρ_{Bulk} [g/mL]	+-	ρ_{Tapped} [g/mL]	+-	P_{HP} [g/mL]	+-	H_R	Ph. Eur. flow character
Syloid® XDP 3050	0.225	0.002	0.287	0.011	2.144	0.004	1.272	Passable
PC on XDP 3050 0.5 mL/g	0.381	0.007	0.460	0.014	1.661 ¹		1.210	Fair
PC on XDP 3050 0.75 mL/g	0.461	0.001	0.553	0.006	1.568 ¹		1.198	Fair
PC on XDP 3050 1 mL/g	0.540	0.012	0.642	0.014	1.508 ¹		1.190	Fair
PC on XDP 3050 1.5 mL/g	0.701	0.005	0.822	0.016	1.432 ¹		1.172	Good
PG on XDP 3050 0.75 mL/g	0.417	0.001	0.511	0.016	1.463 ¹		1.226	Fair
PEG400 on XDP 3050 0.75 mL/g	0.458	0.005	0.550	0.006	1.519 ¹		1.200	Fair
PS80 on XDP 3050 0.75 mL/g	0.436	0.004	0.519	0.005	1.476 ¹		1.190	Fair
Tricalcium citrate tetrahydrate	0.623	0.009	0.682	0.009	1.964	0.001	1.095	Excellent
Pearlitol® 200SD	0.547	0.008	0.595	0.009	1.461	0.002	1.087	Excellent
Vivapur® 101	0.324	0.004	0.467	0.008	1.542	0.001	1.442	Poor
FlowLac® 90	0.572	0.007	0.655	0.003	1.539	0.001	1.145	Good

¹Mathematically calculated values, see equation 2

DOE and Full-Screening Results

The DOE models generally display acceptable R^2 and Q^2 values. Measured tensile strength for optimised mixtures predicted by the DOE, however, showed that tensile strength was severely overestimated by the model (Electronic supplementary information A-2).

To reliably predict tensile strength, the experimental matrix was extended using the same methods already applied in the DOE. Employing the matplotlib library [30] in Python, contour plots (Fig. 1, Electronic supplementary material A3-5) were generated. This approach allowed for the identification of the optimal filler/binder concentration and the optimal compaction pressure for each formulation. Independent of the filler/binder used, all formulations showed some tablet defects, especially at both high and low Liquid Load Levels (Fig. 1, Electronic supplementary material A3-5). With increasing silica content these tablet defects already occurred at lower compaction pressures. At low Liquid Load Levels, delamination was the dominant mode of failure, while at high Liquid Load Levels, most defective tablets had too little mechanical strength to be handled using tweezers.

After analysing all fillers/binders, Vivapur® 101 showed the best performance. It exhibited good tensile strength and high Overall Liquid Load at all tested compaction pressures. Fillers/binders tested, except tricalcium citrate tetrahydrate, had an ideal Liquid Load Level in the range between 0.5 mL/g and 0.8 mL/g (Fig. 2).

Optimised Formulations

According to the full-screening model, the optimal blend to produce liquisolid propylene carbonate tablets was a Liquid

Load Level of 0.75 mL/g, an 80% [v/v] silica content, and Vivapur® 101 as the filler/binder (Fig. 2). After tableting and adjusting the formulation to reach the tensile strength target, the final optimized mixtures can be found in Table II.

Furthermore, optimised mixtures were created for the other fillers/binders with propylene carbonate. For the specific ratios of mixing and compaction pressures refer to Fig. 2. FlowLac® 90 yielded a tensile strength of $1.58(\pm 0.11)$ N/mm² and an Overall Liquid Load of $22.9(\pm 0.1)\%$. Pearlitol® 200SD resulted in tablets with a tensile strength of $1.72(\pm 0.02)$ N/mm² and an Overall Liquid Load of $28.5(\pm 0.1)\%$. Similarly, tricalcium citrate tetrahydrate achieved a tensile strength of $2.21(\pm 0.23)$ N/mm² and an Overall Liquid Load of $18.6(\pm 0.2)\%$.

Compaction Behaviour of Silica and Liquisols Without Binder/Filler

The force–time (Fig. 3a) and pressure–solid fraction data (Fig. 3b) revealed significant changes in the compaction properties of silica at varying Liquid Load Levels. The 0 mL/g and 0.5 mL/g Liquid Load Level silica never exceeded their pycnometric density, while 1.0 mL/g and 1.5 mL/g loaded silica exceeded their helium pycnometer density at low pressure levels of 55 MPa and 25 MPa, respectively. When this limit was surpassed, any additional compression resulted in a swift increase in pressure. The bulk modulus was calculated to be $2.33(\pm 0.08)$ GPa for 1 mL/g silica and $2.44(\pm 0.08)$ GPa for 1.5 mL/g.

At the investigated tableting speed (30 ms dwell time, 650 ms overall compression time), Syloid® XDP 3050 tablets without binder/filler were found to be defective at all Liquid Load Levels. Silica at a low Liquid Load Level tended to burst upon leaving the die (Fig. 4), while those

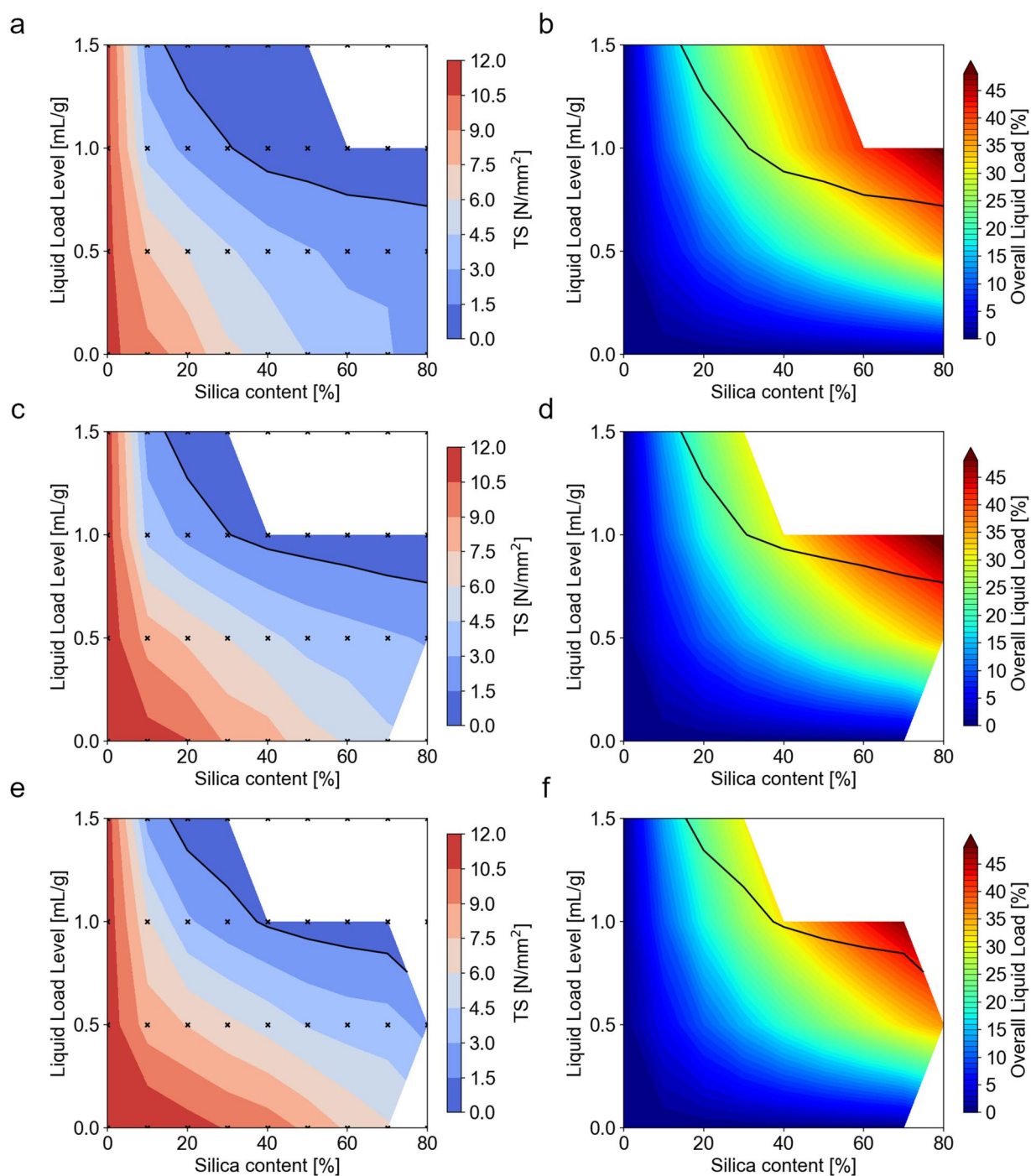


Fig. 1 Python-based presentation and optimisation of tensile strength (TS) and Overall Liquid Load (OLL) for Vivapur® 101/silica mixtures using Matplotlib. White spaces in the graphs represent mixtures producing defective tablets. Each binary mixture is marked with an x. Black TS-target lines are identified in **a** (250 MPa), **c** (350 MPa)

and **e** (450 MPa), respectively and then transferred into OLL-contour plots **b** (250 MPa), **d** (350 MPa) and **f** (450 MPa) for the corresponding pressures. Graphs for other fillers/binders can be found in the electronic supplementary material

with a high Liquid Load Level failed to form any bonds and were too fragile to be handled with tweezers after compression. No external liquid leakage was observed during compression or upon inspection of the tooling

afterwards. Careful transfer and weighing of the very fragile high Liquid Load Level confirmed this, as <1% of the original mass was lost during compression.

Fig. 2 Predicted maximum Overall Liquid Load for a tablet with a predicted tensile strength of 1.5 MPa for all fillers/binders and compaction pressures obtained from Fig. 1. and Figure A3-A5 in the electronic supplementary material. Liquid Load Level and silica content (Sc) for each mixture are given in text under the represented bar

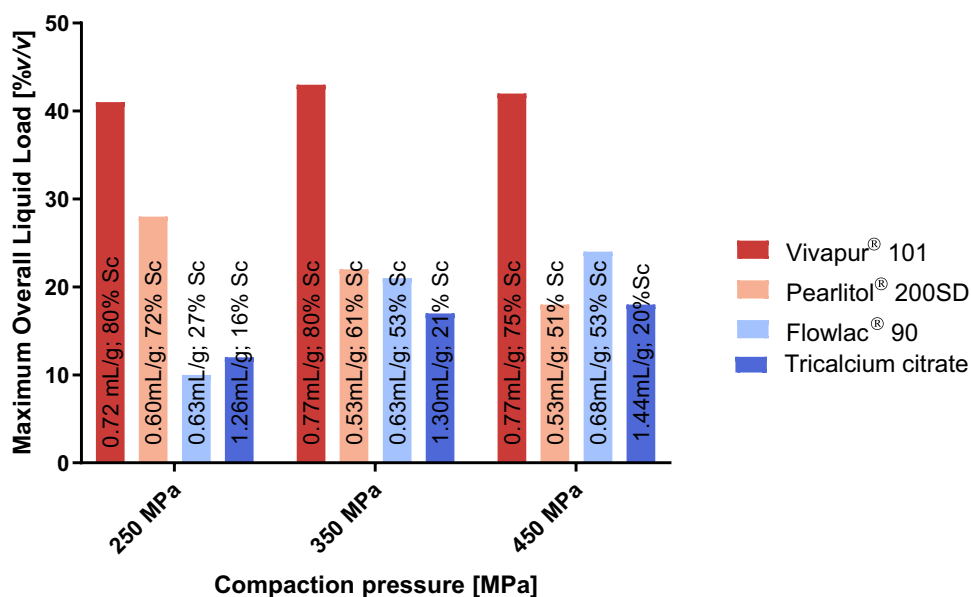


Table II Further optimization of the best combinations, as determined by the Full Screening, with regards to tensile strength (TS) and Overall Liquid Load (OLL). The sample liquids used were propyl-

ene carbonate (PC), propylene glycol (PG), polyethylene glycol 400 (PEG400), and polysorbate 80 (PS 80)

Silica content	80% Silica		70% Silica		65% Silica	
	TS [N/mm ²]	OLL [%]	TS [N/mm ²]	OLL [%]	TS [N/mm ²]	OLL [%]
PC	1.04 ± 0.05	44.8 ± 0.1	1.42 ± 0.05	41.5 ± 0.1	-	-
PG	0.77 ± 0.04	43.8 ± 0.1	1.17 ± 0.05	37.8 ± 0.1	1.61 ± 0.03	35.9 ± 0.1
PEG400	0.96 ± 0.05	45.0 ± 0.1	1.40 ± 0.07	39.9 ± 0.1	-	-
PS 80	1.28 ± 0.06	45.9 ± 0.1	1.50 ± 0.02	39.6 ± 0.1	-	-

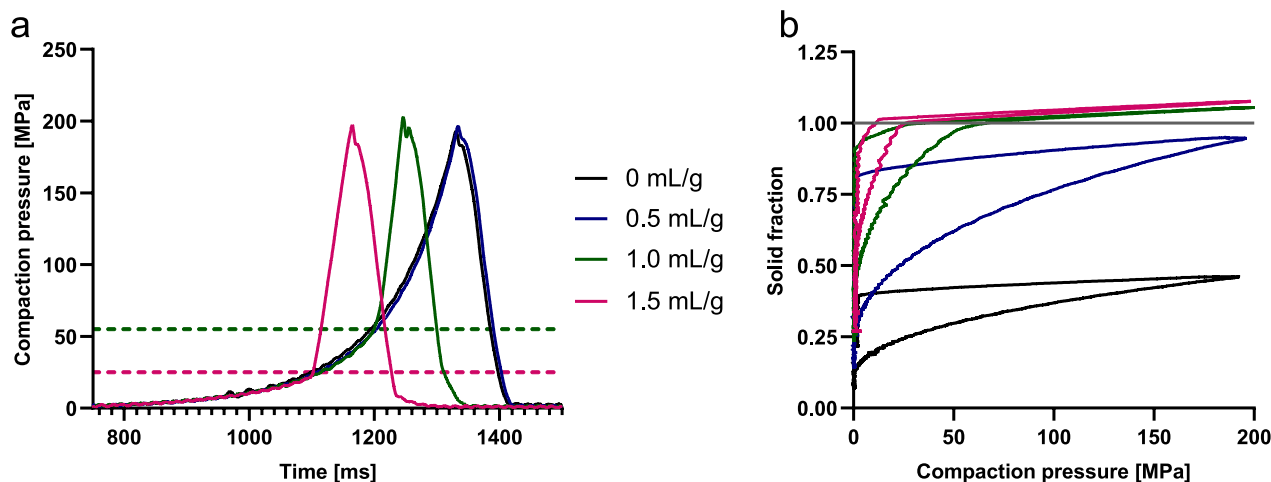


Fig. 3 Compaction behaviour of Syloid XDP 3050 without binder/filler loaded at four Liquid Load Levels utilising the StylOne® default compression cycle at 10% speed; Silica exceeds helium pycnometer density at the dashed lines of their respective colour; 0 mL/g and 0.5 mL/g significantly overlap (a); Solid fraction-compaction pres-

sure curves of Syloid XDP 3050 without binder/filler loaded at four Liquid Load Levels utilising the StylOne® default compression cycle at 10% speed during compression and decompression identifying if/when compacts exceed helium pycnometer density (b)

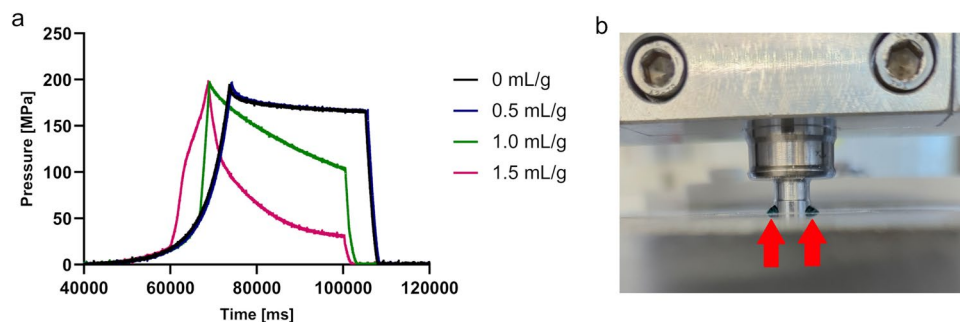
Fig. 4 Syloid® XDP 3050 without binder/filler exploding upon leaving the die after compression at 250 MPa, 10% tableting speed (30 ms dwell time, 650 ms overall compression time)



Extended Dwell Time Measurements

The 30 s dwell time compression cycle was utilised to explore the relaxation behaviour of silica without binder/filler under pressure. Four Liquid Load Levels (0 mL/g, 0.5 mL/g, 1.0 mL/g and 1.5 mL/g) were examined. The silica with Liquid Load Levels of 0 mL/g and 0.5 mL/g quickly experienced a minor pressure decrease of approximately 40 MPa over the first 5 s but remained relatively stable afterwards (Fig. 5a). No external liquid leakage was detected during compression. The plastic flow energy was 198.2(±1.6) mJ for 0 mL/g and 225.5(±12.9) mJ for 0.5 mL/g. Conversely, silica with Liquid Load Levels of 1.0 mL/g and 1.5 mL/g exhibited a higher pressure drop of 100 MPa and 165 MPa and higher plastic flow energies of 563.5(±23.2) mJ and 965.9(±30.0) mJ, respectively (Fig. 5a). Significant external liquid leakage was observed during compression for 1.0 mL/g and 1.5 mL/g, with liquid droplets slowly forming between the die and upper punch (Fig. 5b). Tablets with 0 and 0.5 mL/g Liquid Load Level silica compressed at an extended dwell time did not display any defects, while both higher Liquid Load Level silica tablets were too fragile to be handled with tweezers.

Fig. 5 Force–time data of lissolids and unloaded silica without binder/filler using slow compression and extended dwell times (a); External liquid leakage of methylene blue-dyed propylene carbonate between the upper punch and die-wall (b)



Discussion

As part of our study, the tensile strength was defined as a critical quality attribute and set to a target value of $1.5 \pm 0.1 \text{ N/mm}^2$. Unlike the crushing force, tensile strength is independent of the tablet dimensions [29] making it a critical quality attribute for characterising general tablet strength needed for further processing, packaging and delivery to the customer. The selected target value generally lies between 1.0 and 1.7 N/mm^2 and is dependent on specific process requirements [34]. However, specific requirements or large batches may require higher tensile strength [35]. Very high tensile strength increases disintegration times and is thus undesired for our application [32].

With this study, a new parameter for the loading of a lissolid—the Liquid Load Level [v/m] was introduced. Unlike the Liquid Load Factor [m/m] introduced by Spireas *et al.* [1, 5], the Liquid Load Level is liquid density-independent. This approach allows quick assessment of the total fill level of the silica's pores, as the maximum pore volume is also commonly described on a

volume-per-mass basis [36]. Furthermore, a new critical quality attribute for liquid-solid dosage forms—the Overall Liquid Load [v/v] was defined. This factor describes the liquid volume in a given tablet volume, which is highly relevant for formulation and process development but also from the patient's point of view: The maximum liquid volume, combined with the solubility of the API, limits the maximum dose in a defined tablet volume [37]. As patient compliance decreases significantly with increasing tablet size [38], the reference to the total volume is more relevant than the reference to the tablet mass. Additionally, this approach also enabled easier comparisons between the different fillers/binders used in this study. Otherwise, their differences in density would impact the result if the liquid volume referenced to the total weight of the compact. As such the OLL is not intended as a prediction parameter accessible from a solely mass-based formulation.

This work includes the investigation of binary mixtures which were blended based on bulk volume ratios rather than mass ratios. Syloid® XDP 3050 does not swell when loaded [39], which causes a significant increase in bulk density as the Liquid Load Level increases. If blended based on mass, the resulting mixture would contain fewer silica particles at high Liquid Load Levels despite possessing the same nominal silica content. This event is related to the increased weight of liquid-loaded silica particles. However, this issue can be resolved by bulk volume-based mixing, ensuring that all mixtures with the same nominal silica content contain the same number of particles and, thus, the same potential surface area available for bond formation. Since bonding area and strength are crucial factors in determining a tablet's tensile strength [40–42], the bulk volume ratio provides a more precise description of changes in bonding strength and area for compaction pressure, Liquid Load Level, and silica content than a mass-based approach.

To accurately observe the impact of Liquid Load Level, silica content, and filler/binder type on tensile strength, external lubrication was employed. That is because internal lubrication can affect the tensile strength of different fillers/binders to varying degrees. The effects of internal lubrication on the optimised mixtures were beyond the scope of this investigation.

The compression behaviour of silica and its binary mixtures was highly affected by the Liquid Load Level (Figs. 1., 3a and 5a). The pores of Syloid XDP 3050 have a volume of 1.6 mL/g [23]. The investigated Liquid Load Levels thus covered the entire range from nearly filled to empty pores. The 0 mL/g and 0.5 mL/g Liquid Load Level silica behaved similarly at both slow (30 s dwell time) and fast (0.03 s dwell time) compaction speeds (Fig. 3a, 5a). They only showed a small difference in compaction ratio and plastic flow energy despite the difference in Liquid Load Level. Furthermore, neither showed any external liquid leakage and

both exhibited very similar Kawakita parameters (0.81 and 9.3 vs. 0.80 and 10.9). Both Liquid Load Levels had a high proportion of their pore volume filled with air, explaining the observed differences. The observation that these two Liquid Load Levels behaved similarly and did not show external liquid leakage evidenced that the remaining void space in the pores was preferably expelled during compression. Additionally, the silica with 0.5 mL/g loading was not compressed beyond its pycnometer density (Fig. 3b). This observation is consequential because as the pycnometer density was exceeded, the solid itself could be compressed [43]. With regular solid materials, this results in purely elastic bulk deformation since the solid is immobile. However, in this case, the solid can respond to the densification by releasing the mobile, bound liquid through the gap between the die and the punch after a given lag time. In general, the air inside the pores can also be enclosed during fast compression cycles and reach substantial pressures, which is released during the decompression phase and counteracts the achieved bonding, thus breaking the tablet apart (Fig. 4). Since compression speed is a significant factor for air entrapment-based tablet defects, the effect was less impairing for 0 mL/g and 0.5 mL/g Liquid Load Levels when a very slow compression speed was used [44].

The reason behind the low bonding potential of high Liquid Load Level silica is the fact that even at low compaction pressures of 25–55 MPa, the in-die-density exceeded the helium pycnometer density of the mixture. Upon exceeding the pycnometer density, further compression led to elastic behaviour of the material. If elastic bulk compression of the liquid-solid occurred, it can be assumed that only the liquid component experienced relevant bulk compression, while silica does not get meaningfully compressed [45]. The bulk moduli calculated from the StylOne® default compression cycle at 10% speed ($2.33(\pm 0.08)$ GPa for 1 mL/g; $2.44(\pm 0.08)$ GPa for 1.5 mL/g) closely match the bulk modulus of propylene carbonate found in literature (approx. 2.2 GPa [46]). Theoretically, exceeding the pycnometer density could also be the result of liquid getting squeezed out locally and subsequently being reabsorbed during decompression. A combination of both effects cannot be ruled out as well, emphasising the need for further research of this phenomenon. Exceeding the pycnometer density could lead to two outcomes, depending on the compression speed: Elastic behaviour with no external liquid leakage when compressed quickly (Fig. 3b) or elastic behaviour, followed by external liquid leakage when compressed slowly with extended dwell time (Fig. 5a) [43]. The resulting Kawakita parameters and plastic flow energy values illustrate this effect. Upon exceeding the pycnometer density at lower compaction pressures with increasing Liquid Load Level, the maximum possible degree of compression represented

by the parameter a decreased (from 0 mL/g to 1.5 mL/g: 0.81, 0.80, 0.68, 0.56). The parameter b^{-1} , corresponding with the initial deformation capacity, also decreased substantially (from 0 mL/g to 1.5 mL/g: 9.3, 10.9, 7.54, 4.19). Meanwhile, the plastic flow energy increased, as more liquid got expelled during extended dwell time measurements after the initial inertia was overcome (from 0 mL/g to 1.5 mL/g: 198.2 mJ, 225.5 mJ, 563.5 mJ, 965.9 mJ).

These observations may explain why in most cases tablets with a medium Liquid Load Level and a high silica content outperformed tablets with a high Liquid Load Level and lower silica content in terms of tensile strength and Overall Liquid Load. Medium Liquid Load Level silica represented an optimum at which sufficient air was present in the pores to allow compression without immediately exceeding the pycnometer density and thereby causing elastic behaviour of the material. At the same time the air content is reduced to an adequate level avoiding air entrapment-based tablet defects.

Comparing the DOE contour plots with the full-screening contour plots illustrates that the DOE consistently overestimates the tensile strength at high Liquid Load Levels. At the same time, the DOE underestimated the tensile strength at medium Liquid Load Levels but high silica content (Fig. 6).

The DOE model's poor performance in predicting the tensile strength of liquisolid tablets was likely directly linked to the rapid changes in the tableting properties of their silica content at medium Liquid Load Level. As already explained, capping due to air entrapment [43, 44], is a problem for low Liquid Load Level silica. Likewise, non-existent bonding capacity posed a significant problem at high Liquid Load Levels. Both effects are problematic during tableting (Figs. 1, 4), and the transition between these did not seem to follow a linear pattern. This was illustrated by the similar compaction ratios and Kawakita parameters of 0 mL/g and 0.5 mL/g Liquid Load Level silica on the one hand and the subsequent reduction of these parameters values as Liquid Load Level increased on the other (Table III). The amount of energy available for bond formation was limited by the compression energy, and therefore its normalized form, the compression ratio. Although no precise correlation between the compaction ratio and the actual energy converted into bonding that led to tensile strength could be established, a general relationship between these two parameters was described [47, 48]. In our case, since the compaction ratio dropped sharply, significant changes in bonding strength between 0.5 mL/g, 1.0 mL/g and 1.5 mL/g Liquid Load Level were observed, despite being relatively stable from

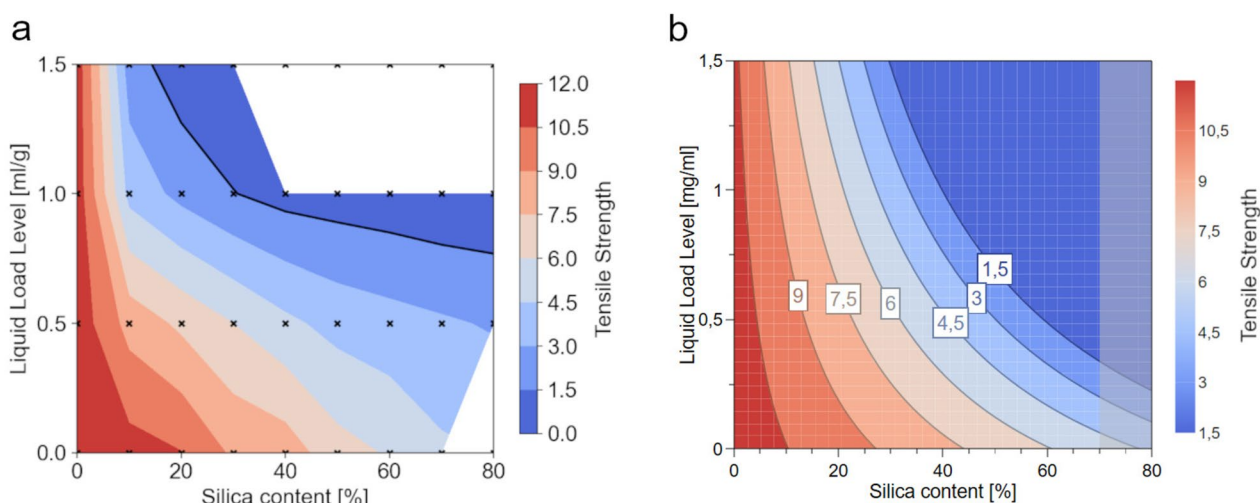


Fig. 6 Comparison of tensile strength predictions by the full-screening model (a) and DOE model (b) with Vivapur® 101 at a compaction pressure of 350 MPa

Table III Kawakita parameters and compaction ratios of pure silica and Liquisolds with varying Liquid Load Levels

Liquid Load Level	Kawakita parameter a	Kawakita parameter b^{-1}	Compaction ratio [%]
0 mL/g	0.81 ± 0.00	9.3 ± 0.2	16.76 ± 0.13
0.5 mL/g	0.80 ± 0.00	10.9 ± 0.1	16.32 ± 0.23
1.0 mL/g	0.68 ± 0.00	7.0 ± 0.4	7.54 ± 0.14
1.5 mL/g	0.56 ± 0.01	2.8 ± 0.5	4.19 ± 0.41

0 mL/g to 0.5 mL/g (Table III). This change in bonding strength, alongside the already discussed air entrapment tendencies, created a complex tensile strength function. The DOE's multilinear regression algorithm did not describe this function adequately, resulting in an incorrect prediction.

While the DOE approach had limitations in tensile strength prediction, the full-screening method yielded better, but still imperfect results (Table IV). While DOE's build their model based on and for the entire dataset, matplotlib's contour prediction model works locally and considers only the nearest four measurement points to predict the contour in each region. This approach may be described as a segmented multilinear model, thus, capturing fast, local changes if sufficient data points are provided. Yet, this process still assumes a linear relationship between these four measurement points and therefore can only approximate a complex function [30, 49]. This approximation limits the accuracy of the segmented multilinear model due to the tensile strength function not being linear, as discussed above. This effect had likely been the reason for deviations observed in our full-screening.

The full-screening method and the DOE achieved good predictability for the Overall Liquid Load of optimised blends (Electronic supplementary material A-2, Table IV). This was not surprising, as the Overall Liquid Load was decisively influenced by the silica content and Liquid Load Level in the binary mixture. Our experiments were designed in a way that these factors increased linearly, allowing both the multilinear regression of the DOE and the segmented multilinear regression of the matplotlib library to accurately predict the Overall Liquid Load. Nonetheless, the solid fraction of the tablets is a factor that may not follow a linear pattern and influences the Overall Liquid Load. Consequently, the segmented multilinear system may offer slightly superior predictive performance compared to the DOE's multilinear system. Results confirmed this, as the Overall Liquid Load

of the optimised propylene carbonate formulation had been predicted more accurately by the segmented multilinear regression.

The production of liquisolid was not limited to propylene carbonate only. There has been a wide use of other liquids, such as propylene glycol [5, 21], PEG400 [8, 19, 50, 51] or polysorbate 80 [20, 52]. It was, therefore, interesting to apply the optimum of 0.75 mL/g Liquid Load Level, 80% silica content and 350 MPa found for propylene carbonate and Vivapur® 101 to these other liquids. The results of tensile strength tests showed differences between the four liquids tested, but these differences were minor in absolute values. There are also small differences between the four liquids regarding the Overall Liquid Load of the respective tablets. Our results indicate that the influence of liquid type was relatively minor compared to other factors, such as the Liquid Load Level or the silica content. This observation allows the discovered optimum to be easily adapted to other liquid formulations, as only a few modifications of the silica content were sufficient to optimise tensile strength and Overall Liquid Load for four chemically diverse liquid components.

In terms of filler/binder performance, Vivapur® 101 was ranked as the top-performing filler/binder, explained by its well-known tabletability and versatility [53]. Since its selection as a carrier material for liquids in many liquisolid systems, it has already shown its capacity to form bonds, even when directly used as a carrier for the liquid component [5]. Meanwhile, Pearlitol® 200SD, regarded a less plastic material than Vivapur® 101 [54], outperformed the purely brittle deforming tricalcium citrate tetrahydrate and FlowLac® 90, even as tricalcium citrate tetrahydrate usually exhibits much higher tabletability. FlowLac® 90 likewise outperforms tricalcium citrate tetrahydrate, though it is generally inferior in tabletability [55]. FlowLac® 90 consists of brittle α -lactose monohydrate and plastic amorphous lactose. The

Table IV Comparison between optimised formulations with a specified Liquid Load Level (LLL), silica content (Sc), compaction pressure (P), tensile strength (TS) and Overall Liquid Load (OLL) pre-

dicted by DOE and full-screening, as well as the actual values measured from these formulations

Method	Material	Model Prediction					Actual Value	
		LLL [mL/g]	Sc [%]	P [MPa]	TS [N/mm ²]	OLL [%]	TS [N/mm ²]	OLL [%]
DOE	Vivapur® 101	1.5	30	350	1.5	33.5	0.31	30.8
	FlowLac® 90	1.5	20	450	1.5	17.9	0.29	16.8
	Pearlitol® 200SD	1.5	20	450	1.47	15.9	0.30	15.7
	Tricalcium citrate tetrahydrate	1.5	20	450	1.49	19.9	1.21	19.5
Full- Screening	Vivapur® 101	0.75	80	350	1.5	43	1.04	44.8
	FlowLac® 90	0.68	50	450	1.5	24	1.58	22.9
	Pearlitol® 200SD	0.60	70	250	1.5	28	1.72	28.5
	Tricalcium citrate tetrahydrate	1.4	20	450	1.5	18	2.21	18.6

deformation behaviour is mainly characterised by its brittle α -lactose monohydrate crystals, while the binding behaviour is mainly influenced by its plastic amorphous lactose content [56]. These observations imply the superiority of plastic deformable fillers/binders for this application, as the plastic fillers/binders outperformed the partially plastic FlowLac® 90 and brittle tricalcium citrate tetrahydrate.

The final optimum found by the full-screening and subsequent further optimisation was a binary mixture of 70 volume parts 0.75 mL/g Liquid Load Level Syloid® XDP 3050 and 30 volume parts Vivapur® 101 compressed at 450 MPa. Regarding the practical application of this mixture, such as formulation of a liquid plant extract or new chemical entity as an alternative to soft encapsulation, some limitations of our study must be considered. To properly analyse the interaction between silica and binder, we used external lubrication and did not include any other additives such as disintegrants. Furthermore, although this study was conducted on a compression simulator, we did not analyse the influence of different compression profiles or speeds. All these factors should be analysed in the future to develop the found optimum into a platform technology that allows for a cheap, reliable and rapid formulation of high dose tablets, containing different liquid formulations or APIs.

Conclusion

Our research introduced a critical quality attribute for liquisolid, the Overall Liquid Load. It describes the volume of liquid per tablet volume and is a patient and formulation-relevant factor that enables simple comparison between different liquisolid formulation strategies and varying formulation compositions. Furthermore, our study demonstrated Syloid® XDP 3050s challenging compression characteristics and the need for adding a high plasticity filler/binder with strong binding capacity when formulated into tablets. The use of plastic fillers/binders in tablet formulation is recommended for both loaded and unloaded Syloid® XDP 3050. To identify the most appropriate filler/binder, a systematic analysis by testing binary blends of various silica contents at various Liquid Loading Levels with four different fillers/binders using a DOE and a full-screening approach was conducted. The DOE approach was found to be inadequate due to non-linear tensile strength behaviour. The full-screening identified Vivapur® 101 as the optimal filler/binder. It allowed for the highest possible Overall Liquid Load, while maintaining an acceptable tensile strength. The found optimum of 70% silica content at a Liquid Load Level of 0.75 mL/g and 30% Vivapur® 101, using 450 MPa of compaction pressure, allowed to produce tablets with > 40% Overall Liquid Load (propylene carbonate), while maintaining a tensile strength of 1.5 N/mm². This optimum is

transferable to multiple other liquid components with minimal adaptation and can thus serve as a general concept, producing high drug-load liquisolid tablets.

Supplementary Information The online version contains supplementary material available at <https://doi.org/10.1208/s12249-024-02958-9>.

Acknowledgements The authors would like to express their gratitude to Romaco Kilian GmbH and Medelpharm S.A.S. for generously providing the StylOne® Classic single punch compression simulator. Additionally, we extend our thanks to Mathias Hücke Software for providing the Tab-Fox® Analyser software. We are also grateful to Marvin Brenner and Safiye Rafehi for their valuable feedback on this manuscript.

Author Contributions Conceptualisation: K.G.W, K.E.S and J.A; Data curation: J.A; Methodology: J.A., K.E.S and K.G.W; Investigation: J.A; Resources: K.G.W; Writing-Original Draft Preparation: J.A; Writing-Review and Editing: K.E.S and K.G.W; Supervision: K.G.W; Project Administration: K.G.W

Funding Open Access funding enabled and organized by Projekt DEAL. This research did not receive any specific grant from funding agencies in the public, commercial, or not-for-profit sectors.

Declarations

Conflict of interest The authors declare no conflict of interest.

Open Access This article is licensed under a Creative Commons Attribution 4.0 International License, which permits use, sharing, adaptation, distribution and reproduction in any medium or format, as long as you give appropriate credit to the original author(s) and the source, provide a link to the Creative Commons licence, and indicate if changes were made. The images or other third party material in this article are included in the article's Creative Commons licence, unless indicated otherwise in a credit line to the material. If material is not included in the article's Creative Commons licence and your intended use is not permitted by statutory regulation or exceeds the permitted use, you will need to obtain permission directly from the copyright holder. To view a copy of this licence, visit <http://creativecommons.org/licenses/by/4.0/>.

References

1. Spireas SS, Jarowski CI, Rohera BD. Powdered Solution Technology: Principles and Mechanism. *Pharm Res.* 1992;9(10):1351–8.
2. Sun WJ, Aburub A, Sun CC. A mesoporous silica based platform to enable tablet formulations of low dose drugs by direct compression. *Int J Pharm.* 2018;539(1–2):184–9.
3. McCarthy CA, Ahern RJ, Dontireddy R, Ryan KB, Crean AM. Mesoporous silica formulation strategies for drug dissolution enhancement: a review. *Expert Opin Drug Deliv.* 2016;13(1):93–108.
4. Linnell T, Santos HA, Mäkilä E, Heikkilä T, Salonen J, Murzin DYU, et al. Drug Delivery Formulations of Ordered and Nonordered Mesoporous Silica: Comparison of Three Drug Loading Methods. *J Pharm Sci.* 2011;100(8):3294–306.
5. Spireas S, inventor; Liquisolid systems and methods of preparing same. United States patent US6423339B1, 2002 [cited 2023 Oct 12]. Available from: <https://patents.google.com/patent/US6423339B1/en>
6. Lipinski CA, Lombardo F, Dominy BW, Feeney PJ. Experimental and computational approaches to estimate solubility and

- permeability in drug discovery and development settings IPII of original article: S0169-409X(96), 00423-1. *Adv Drug Deliv Rev.* 1997;23(1):3-25 (2001 Mar 1;46(1):3-26).
7. Tabboon P, Pongjanyakul T, Limpongsa E, Jaipakdee N. In Vitro Release, Mucosal Permeation and Deposition of Cannabidiol from Liquisolid Systems: The Influence of Liquid Vehicles. *Pharmaceutics.* 2022;14(9):1787.
 8. Tiong N, Elkordy AA. Effects of liquisolid formulations on dissolution of naproxen. *Eur J Pharm Biopharm.* 2009;73(3):373-84.
 9. Akinlade B, Elkordy AA, Essa EA, Elhagar S. Liquisolid Systems to Improve the Dissolution of Furosemide. *Sci Pharm.* 2010;78(2):325-44.
 10. Javadzadeh Y, Jafari-Navimipour B, Nokhodchi A. Liquisolid technique for dissolution rate enhancement of a high dose water-insoluble drug (carbamazepine). *Int J Pharm.* 2007;341(1):26-34.
 11. Elkordy AA, Tan XN, Essa EA. Spironolactone release from liquisolid formulations prepared with Capryol™ 90, Solutol® HS-15 and Kollicoat® SR 30 D as non-volatile liquid vehicles. *Eur J Pharm Biopharm.* 2013;83(2):203-23.
 12. Spireas S, Sadu S. Enhancement of prednisolone dissolution properties using liquisolid compacts. *Int J Pharm.* 1998;166(2):177-88.
 13. Hentzschel CM, Alnaief M, Smirnova I, Sakmann A, Leopold CS. Enhancement of griseofulvin release from liquisolid compacts. *Eur J Pharm Biopharm.* 2012;80(1):130-5.
 14. Khaled KA, Asiri YA, El-Sayed YM. In vivo evaluation of hydrochlorothiazide liquisolid tablets in beagle dogs. *Int J Pharm.* 2001;222(1):1-6.
 15. Badawy MA, Kamel AO, Sammour OA. Use of biorelevant media for assessment of a poorly soluble weakly basic drug in the form of liquisolid compacts: in vitro and in vivo study. *Drug Deliv.* 2016;23(3):808-17.
 16. Hentzschel CM, Sakmann A, Leopold CS. Suitability of various excipients as carrier and coating materials for liquisolid compacts. *Drug Dev Ind Pharm.* 2011;37(10):1200-7.
 17. Liao CC, Jarowski CI. Dissolution rates of corticoid solutions dispersed on silicas. *J Pharm Sci.* 1984;73(3):401-3.
 18. Lamprecht A, Grizic D, inventors; Pharmaceutical formulations using propylene carbonate. German patent DE102015008534A1, 2017 [cited 2023 Oct 12]. Available from: <https://patents.google.com/patent/DE102015008534A1/en>
 19. Yadav V, Yadav A. Enhancement of solubility and dissolution rate of BCS class II pharmaceuticals by nonaqueous granulation technique. *Int J Pharma Res Dev-Online.* 2010;1:1.
 20. Javadzadeh Y, Siahi MR, Asnaashari S, Nokhodchi A. An Investigation of Physicochemical Properties of Piroxicam Liquisolid Compacts. *Pharm Dev Technol.* 2007;12(3):337-43.
 21. Gubbi S, Jarag R. Liquisolid Technique for Enhancement of Dissolution Properties of Bromhexine Hydrochloride. *Res J Pharm Technol.* 2009;2(2):382-6.
 22. Lam M, Ghafourian T, Nokhodchi A. Liqui-Pellet: the Emerging Next-Generation Oral Dosage Form Which Stems from Liquisolid Concept in Combination with Pelletization Technology. *AAPS PharmSciTech.* 2019;20(6):231.
 23. Choudhari Y, Reddy U, Monsuur F, Pauly T, Hoefer H, McCarthy W. Comparative evaluation of porous silica based carriers for lipids and liquid drug formulations. *Open Mater Sci.* 2014;1(1). Available from: <https://www.degruyter.com/document/doi/10.2478/mesbi-2014-0004/html>
 24. Lam M, Ghafourian T, Nokhodchi A. Liquisolid System and Liqui-Mass System Are Not the Same. *AAPS PharmSciTech.* 2020;21(3):105.
 25. Pezzini BR, Berings AO, Ferraz HG, Silva MAS, Stulzer HK, Sonaglio D. Liquisolid Pellets and Liqui-Pellets Are Not Different. *AAPS PharmSciTech.* 2020;21(2):72.
 26. Lu M, Xing H, Jiang J, Chen X, Yang T, Wang D, et al. Liquisolid technique and its applications in pharmaceuticals. *Asian J Pharm Sci.* 2017;12(2):115-23.
 27. Wagner KG, Lamprecht A, Krome AK, Grizic D, Becker T, inventors; Liquisolid pharmaceutical formulation and process for manufacturing. European patent EP 3 903 770 A1.
 28. European Pharmacopoeia. 10th ed. Deutscher Apotheker Verlag; 2019.
 29. Fell JT, Newton JM. Determination of Tablet Strength by the Diametral-Compression Test. *J Pharm Sci.* 1970;59(5):688-91.
 30. Hunter JD. Matplotlib: A 2D Graphics Environment. *Comput Sci Eng.* 2007;9(3):90-5.
 31. Kawakita K, Lüdde KH. Some considerations on powder compression equations. *Powder Technol.* 1971;4(2):61-8.
 32. Alderborn G, Nyström C. Pharmaceutical powder compaction technology. Marcel Dekker; 1996.
 33. Nordström J, Klevan I, Alderborn G. A Particle Rearrangement Index Based on the Kawakita Powder Compression Equation. *J Pharm Sci.* 2009;98(3):1053-63.
 34. Pitt KG, Heasley MG. Determination of the tensile strength of elongated tablets. *Powder Technol.* 2013;1(238):169-75.
 35. Sabri AH, Hallam CN, Baker NA, Murphy DS, Gabbott IP. Understanding tablet defects in commercial manufacture and transfer. *J Drug Deliv Sci Technol.* 2018;1(46):1-6.
 36. Xi Y, Liangying Z, Sasa W. Pore size and pore-size distribution control of porous silica. *Sens Actuators B Chem.* 1995;25(1):347-52.
 37. Burra S, Yamsani M, Vobalaboina V. The Liquisolid technique: an overview. *Braz J Pharm Sci.* 2011;47:475-82.
 38. Hummler H, Stillhart C, Meilicke L, Grimm M, Krause E, Manana M, et al. Impact of Tablet Size and Shape on the Swallowability in Older Adults. *Pharmaceutics.* 2023;15(4):1042.
 39. W.R. Grace. SYLOID® XDP silica for conversion of oily actives into powders. 2020 [cited 2023 Nov 7]. Available from: <https://www.youtube.com/watch?v=KsfBYL-7mGQ>
 40. Nyström C, Alderborn G, Duberg M, Karehill PG. Bonding Surface area and Bonding Mechanism—Two Important Factors for the Understanding of Powder Comparability. *Drug Dev Ind Pharm.* 1993;19(17-18):2143-96.
 41. Osei-Yeboah F, Chang SY, Sun CC. A critical Examination of the Phenomenon of Bonding Area - Bonding Strength Interplay in Powder Tableting. *Pharm Res.* 2016;33(5):1126-32.
 42. Leuenberger H, Jetzer W. The compactibility of powder systems - a novel approach. *Powder Technol.* 1984;37(1):209-18.
 43. Schönfeld BV, Westedt U, Wagner KG. Compression Modulus and Apparent Density of Polymeric Excipients during Compression—Impact on Tabletability. *Pharmaceutics.* 2022;14(5):913.
 44. Klinzing GR, Troup GM. Modeling the Air Pressure Increase Within a Powder Bed During Compression—A Step Toward Understanding Tablet Defects. *J Pharm Sci.* 2019;108(6):1991-2001.
 45. *Elastic Moduli Data for Polycrystalline Ceramics*, R. G. Munro, NISTIR 6853. National Institute of Standards and Technology, Gaithersburg, Maryland 20899. 2022. Available from: <https://srdata.nist.gov/CeramicDataPortal/Elasticity/SiO2>
 46. Lyapin AG, Gromnitskaya EL, Danilov IV, Brazhkin VV. Elastic properties of the hydrogen-bonded liquid and glassy glycerol under high pressure: comparison with propylene carbonate. *RSC Adv.* 2017;7(53):33278-84.
 47. Çelik M. Overview of Compaction Data Analysis Techniques. *Drug Dev Ind Pharm.* 1992;18(6-7):767-810.
 48. Çelik M, Marshall K. Use of a Compaction Simulator System in Tableting Research. *Drug Dev Ind Pharm.* 1989;15(5):759-800.
 49. Thomas I. Algorithm description - ContourPy documentation. [cited 2023 Oct 19]. Available from: <https://contourpy.readthedocs.io/en/v1.1.1/description.html>

50. Mamidi HK, Mishra SM, Rohera BD. Determination of maximum flowable liquid-loading potential of Neusilin® US2 and investigation of compressibility and compactibility of its liquisolid blends with PEG (400). *J Drug Deliv Sci Technol*. 2019;1(54):101285.
51. Molaei MA, Osouli-Bostanabad K, Adibkia K, Shokri J, Asnaashari S, Javadzadeh Y. Enhancement of ketoconazole dissolution rate by the liquisolid technique. *Acta Pharm*. 2018;68(3):325–36.
52. El-Houssieny BM, Wahman LF, Arafa NMS. Bioavailability and biological activity of liquisolid compact formula of repaglinide and its effect on glucose tolerance in rabbits. *Biosci Trends*. 2010;4(1):17–24.
53. Thoorens G, Krier F, Leclercq B, Carlin B, Evrard B. Microcrystalline cellulose, a direct compression binder in a quality by design environment—A review. *Int J Pharm*. 2014;473(1):64–72.
54. Li XH, Zhao LJ, Ruan KP, Feng Y, Xu DS, Ruan KF. The application of factor analysis to evaluate deforming behaviors of directly compressed powders. *Powder Technol*. 2013;1(247):47–54.
55. Hagelstein V, Gerhart M, Wagner KG. Tricalcium citrate – a new brittle tableting excipient for direct compression and dry granulation with enormous hardness yield. *Drug Dev Ind Pharm*. 2018;44(10):1631–41.
56. Vromans H, Bolhuis GK, Lerk CF, van de Biggelaar H, Bosch H. Studies on tableting properties of lactose. VII. The effect of variations in primary particle size and percentage of amorphous lactose in spray dried lactose products. *Int J Pharm*. 1987;35(1):29–37.

Publisher's Note Springer Nature remains neutral with regard to jurisdictional claims in published maps and institutional affiliations.